INFLUENCE OF THE PROJECTILE SHAPE ON THE DYNAMIC TENSILE CHARACTERIZATION OF CONCRETE USING A SPLIT HOPKINSON BAR

MARIA L. RUIZ-RIPOLL[1], VICTOR REY DE PEDRAZA[2] & CHRISTOPH ROLLER[1]
[1]Fraunhofer Institute for High-Speed Dynamics, Ernst-Mach Institut (EMI), Germany
[2]Departamento de Ciencia de los Materiales, ETSI Caminos, Canales y Puertos, Universidad Politécnica de Madrid, Spain

ABSTRACT

Because of its relevance in civil infrastructures, the analysis of the dynamic behaviour of concrete has increased exponentially in recent years. This is motivated by the new type of threats that have to be taken into consideration nowadays when designing these types of structures. The growing interest in the dynamic response of concrete arises from the enhancement of its mechanical properties when the material is subjected to high strain rates. In this research, the traditional Split Hopkinson Pressure Bar developed by Kolsky, with a standard compression configuration (including incident and transmitted bars) was modified into a version in which the transmission bar was removed, so that the specimen's response is dominated by tensile stresses inside it. Spalling tests on cylindrical samples were carried out to measure the tensile strength and the fracture energy of conventional concrete. Results for strain rates ranging from 60 to 130 s^{-1} are presented and compared to the respective quasi-static values. As the key point of the research, two different projectile shapes (cylindrical and conical) have also been evaluated, presenting a qualitative and quantitative analysis regarding the variations in tensile stress evolution of the pulses.

Keywords: Split Hopkinson Bar, spalling, dynamic tensile strength, concrete, fracture.

1 INTRODUCTION

The use of the Split Hopkinson Bar (SHB) technique for testing materials subjected to high strain rates has increased notably during the last decades, based on the number of related publications [1]. The interest shown by many researchers in the use of this technique to obtain different material mechanical properties can be appreciated in the variety of test configurations employed. Varying from compression and tensile tests in rocks [2] and concrete [3], compression to tensile testing in metals [4], to most recent 3D configurations to study more complex events [5], this versatility makes the SHB a very powerful tool with many possibilities ahead.

Because of its relevance in civil infrastructures, the analysis of the dynamic behaviour of concrete has increased exponentially during the recent years, researchers are prompted by the new type of threats that nowadays menaces these types of structures. Terrorist attacks, natural disasters, or accidents impulsed researchers to understand the behaviour of concrete under such events. The growing interest in the study of the dynamic response of concrete originates from the enhancement of the mechanical properties when concrete materials are subjected to high strain rates [6] which are still attracting many researchers [7]. For analysing the dynamic behaviour of materials, the traditional Split Hopkinson Pressure Bar device, developed by Kolsky [8] (with the incident and transmitted bars, typically used for studying compressive behaviours) was modified into a version in which the transmission bar was removed, so that the specimen's response is dominated by tensile stresses inside it [9]. This modification opened up a large new field of possibilities on the testing configurations, leading to new several data analysis techniques too. First works came during the 1980s [6], [10], [11], with some important contributions in the 1990s [12], and most recently works

WIT Transactions on The Built Environment, Vol 209, © 2022 WIT Press
www.witpress.com, ISSN 1743-3509 (on-line)
doi:10.2495/HPSU220141

[13]–[16]. However, the complexity of the process of analysis of the results is not an easy task. Variations in the length, geometry, or material of the bars, instrumentation, recording system, and differences in the launch system allow the possibility of a broad range of results and interpretations. The projectile geometry can play an important role on the dynamic characterization of the materials. Based on the work of Gálvez Díaz-Rubio et al. [17] and Rey de Pedraza et al. [18] this work aims to present the influence of two projectile shapes on the determination of the dynamic properties of concrete.

The paper presents the results from a collaboration work between the Polytechnical University of Madrid (UPM) and Fraunhofer EMI. The influence of the projectile geometry (cylindrical and conical shaped) is evaluated for spallation experiments on cylindrical concrete specimens. The experiments are performed in a modified Split Hopkinson Bar at different strain rates. The work presents a quantitative and qualitative analysis concerning the variation in tensile stress evolution of the pulses.

2 EXPERIMENTAL PROGRAM

2.1 Specimen manufacturing

Samples for the dynamic campaign, consisting of concrete cylinders of 75 mm diameter and 300 mm length, were directly obtained by drilling into a uniform concrete block of dimensions 1000 × 300 × 250 mm^3. The drilling of specimens from a large block allows obtaining a very homogeneous mixture for every specimen and avoids the problem of vibration of slender specimens and the wall effect.

The concrete mix was designed by an extern company under the requirements of compressive strength of 50 MPa.

2.2 Quasi-static characterisation

To know the quasi-static behaviour of the concrete mixture, quasi-static compression, Brazilian, and three-point-bending (TPB) tests were conducted. Two specimens per test configuration were performed, the results were averaged and are shown in Table 1. Standard compression and Brazilian tests were performed following the standard specifications [19].

Table 1: Averaged quasi-static concrete properties. Standard deviation (%) in brackets.

Concrete properties	M1	M2	Mean
Density (kg/m^3)	2,288	2,324	2,306 (25)
σ_c (MPa)	65	66.3	65.7 (0.9)
f $_t$ (MPa)	5.2	4.3	4.8 (0.6)
G $_F$ (kN/mm)	3.5E-4	2.5E-4	3.0E-4 (7.0E-5)
c $_{concrete}$ (m/s)	3,800	3,802	3,801 (1)
E $_{dyn}$ (GPa)	33.3	33.3	33.3 (0)

The quasi-static TPB tests were performed as described in RILEM [20], but using cylindrical notched specimens. The total fracture energy (E_F) was then determined using numerical integration of the force-displacement curve, and the area under them. The specific fracture energy (G_F) is derived by dividing the fracture area (A_F), which represents the consumed energy during the fracture process.

2.3 Dynamic test setup

Dynamic spalling tests were carried out, using a modified configuration from the standard compression configuration from a Split Hopkinson Bar [8], (Fig. 1). In the spalling configuration, there is no transmission bar, so the specimen's response is dominated by tensile stresses inside it.

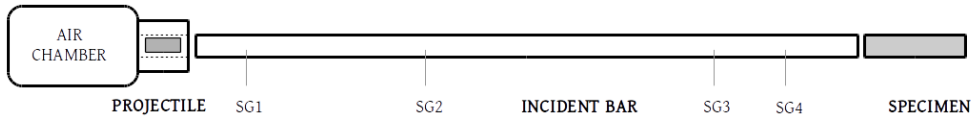

Figure 1: Experimental scheme of the SHB device.

The used SHB device is composed of an aluminium incident bar with 75 mm diameter and 5,500 mm length, and a steel projectile with a length of 60 mm. The projectile (cylindrical or conical shaped) is disposed inside air cannon. The concrete specimen is glued to the incident bar. Strain gauges are displaced along the incident bar and the specimen, tracking the evolution of the wave.

The versatility of the presented configuration has been proved at EMI for several materials. Among others on sedimentary rocks [21], or on high-performance concrete mixes [22].

3 INFLUENCE OF THE PROJECTILE SHAPE

Two different projectile geometries are analysed in this work based on the modification of the classical cylindrical projectile geometry made by Gálvez Díaz-Rubio et al. [17] and Rey de Pedraza et al. [18]. When using cylindrical projectiles with a high length/diameter ratio, the pulse generated can be assumed to be rectangular, as seen in Fig. 2(a). The typical rising part to the constant compression level is modified when the projectile shape changes. Following the work of Kolsky and Shi [23], the use of triangular pulse leads to some advantages after the reflection of the compressive pulse: the stress evolution after reflection follows a gradual increase instead of a sudden rising (Fig. 2(b)), and fewer sections would be simultaneously subjected to equivalent tensile stress.

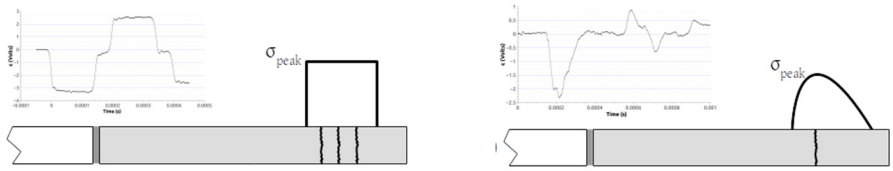

(a) (b)

Figure 2: Differences in the pulse shapes based on the projectile geometry. (a) Cylindrical projectile; and (b) Conical projectile.

Based on the existing cylindrical projectile, the dimensions of the conical one were defined. Furthermore, before manufacturing it, the behaviour of the two different shapes were validated by using LS-Dyna code. The conical shape projectile was therefore adjusted to the

restrains of length and major face diameter of 60 mm (Fig. 3(a)), preserve of impact energy, and the use of polymer sabot (where projectile core is embedded). A comparison between experimental and numerical obtained pulses for both geometries is presented in Fig. 3(b). Conical projectile pulse has a more regular pulse branch in comparison with the disturbed branch of the cylindrical one. By reducing the diameter of the reflecting face of the projectile leads to shorter time-pulses, and therefore to a smaller portion of the sample affected by the superimposition of the waves.

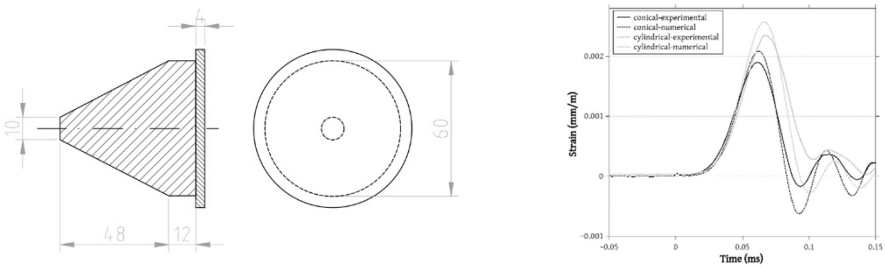

(a) (b)

Figure 3: (a) Conic projectile's geometry (dimensions in mm); and (b) Experimental and numerical comparison of the pulse shapes.

4 DATA ANALYSIS APPROACH

The estimation of the tensile strength or the fracture energy required two different configurations of specimens. The difference between them is the use of notched specimens for fracture energy analysis (Fig. 4). Having a notched specimen promotes a single fracture in the specimen, avoiding or reducing the possibility of having multiple fractures as, thanks to the area reduction at the notch, tensile stresses can be kept below the dynamic tensile strength of concrete in every section outside the notch.

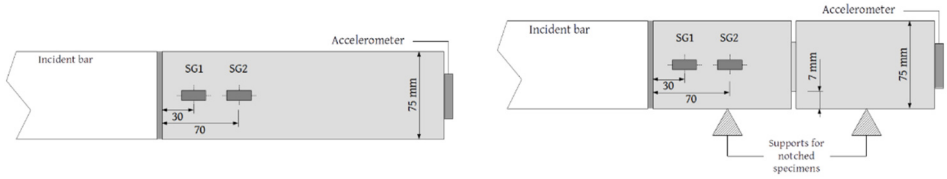

(a) (b)

Figure 4: (a) Tensile test specimen configuration; and (b) Energy tests specimen configuration.

In the tensile configuration the specimen was glued to the incident bar using an epoxy resin. For the fracture energy configuration, the specimen is not glued but linked to it using a mortar mix, enough to transmit the compressive pulse from the incident bar to the specimen. The applied methodology (see Section 4.2) requires that all the specimen's parts are free to be ejected after the fracture occurs, so the momentum of each ejected piece of the concrete specimen can be accurately measured which results in a better approximation of the fracture energy. Extra supports are then needed under the specimen, as shown in Fig. 4, to withstand

the self-weight of concrete. Two strain gauges are used in both configurations however, the need for two different records for the strains has a special relevance in the case of the energy tests where initial and residual strains inside the concrete specimen have to be recorded at different points to avoid superposition of the pulses.

4.1 Tensile strength

During the spalling test, the projectile is ejected against the incident bar at different air pressures. This pressure influences the stress peak and so the strain rate on the specimen. The tensile strength is derived by using the Novikov approach [24], based on

$$f_{t,dyn} = \frac{1}{2}\rho \cdot c_L \cdot \Delta u_{pb} \tag{1}$$

where the density (ρ) and wave speed (c_L) of concrete and the so-called pullback velocity (Δu_{pb}) of the ejected end of the specimen are used to estimate the tensile strength. The wave speed can be measured thanks to the recorded signals of one of the strain gauges and the accelerometer (see Fig. 4). As the position of both of them is known and the difference in the arrival time is given by the signal records, the wave speed can be directly computed. The pullback velocity can be defined as the difference in velocities of the free end before and after the spallation occurs and is a kinematic approximation of the loss of energy during the fracture process (see Fig. 5). Thus, the dynamic young modulus (E_{dyn}) is derived from the expressions of the theory of unidimensional wave propagation on elastic materials by

$$E_{dyn} = \rho \cdot c_L^2 \tag{2}$$

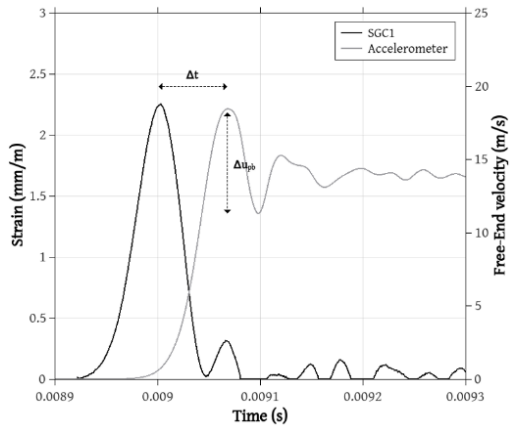

Figure 5: Signal records at the strain gauge and accelerometer.

4.2 Fracture energy

For the analysis of the dynamic fracture energy, the dynamic tensile configuration is modified at some points. First, the use of notched specimens, is required to promote a single and located fracture in the specimen where the area reduction leads to a higher stress level compared to the rest of the sections, ensuring that a fracture is going to occur at that point. Second, the notched specimen is not glued to the incident bar as already commented at the beginning of Section 4.

The dynamic fracture energy was derived by using the Momentum approach, proposed by Schuler et al. [25]. One of the critical factors of this technique is that in notched specimens after the fracture occurs, the formed pieces are ejected freely so that the velocities, and thus the momentum, can be accurately measured. The velocity of the fragments can then be measured by using different sensors, such as digital extensometers, accelerometers or digital image correlation (DIC). As the mass of the separated fragments can be measured after the test, the moment of inertia can be easily computed.

The estimation of the fracture energy (G_F) is derived from different parameters as the momentum transfer between fragments (ΔI), the solid rigid velocity of the ejected free end, before ($v_2(t_1)$) and after fracture occurs ($v_2(t_2)$), and the crack opening velocity ($\dot{\delta}$). The authors suggest to visit Schuler et al. [25] paper for the complete approach details.

5 RESULTS

5.1 Tensile tests

Tensile tests were performed using both projectiles under three different air pressures. For each pressure (0.5, 1.0 and 1.5 bar) two experiments were conducted. Fig. 6 displays the evolution of strain rates as a function of the pressures, reaching strain rates ranging from 60 s^{-1} to 130 s^{-1}. It can be seen how the influence of the projectile shape on the strain rate is minimal, as the strain rates till the spalling moment are very similar for both geometries.

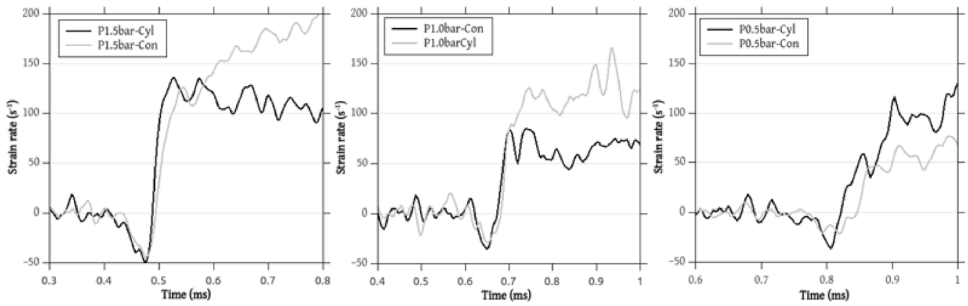

Figure 6: Evolution of the strain rates during spalling test at different pressures tested (from left to right 1.5, 1.0 and 0.5 bar).

Tensile strenght together with other important parameters are presented in Table 2. The results show uniformity and coherence on the values for all the strain rates analyzed. As expected, the Dynamic Increase Factor (DIF) increase with the strain rate, reaching a value close to 7 at a strain rate of 125 s^{-1}.

An analysis of the fracture pattern was made for a qualitative point of view, comparing the numer and spacing of fractures as a function of the projectile shape and strain rate (see Fig. 7). Specimen tested with the cylindrical projectile presented more damage in comparison to the conical ones. Even when the strain rates where similar for both projectile under same pressure, the specimens tested with the cylindrical projectile displayed a higher density of fractures. The evolution of the facture position, as well as partial opened cracks is more gradual and controlled in the specimens where conical projectile was used. Therefore and based on the fracture patterns, it is convenient the use of conical projectile for spalling test.

Table 2: Dynamic tensile strength results.

#Test	P (bar)	$\dot{\varepsilon}$ (s^{-1})	v_{min}(m/s)	v_{max} (m/s)	u_{pb} (m/s)	σ (MPa)	DIF_{f_t}
Cyl1	1.5	130	11.30	18.46	7.14	31.3	6.5
Cyl2	1.0	88	12.50	18.40	5.86	25.7	5.3
Cyl3	0.5	60	6.24	10.15	3.91	17.1	3.6
Con1	1.5	125	7.00	14.43	7.43	32.6	6.8
Con2	1.0	83	7.20	12.97	5.77	25.3	5.3
Con3	0.5	50	5.18	7.56	2.38	10.4	2.2

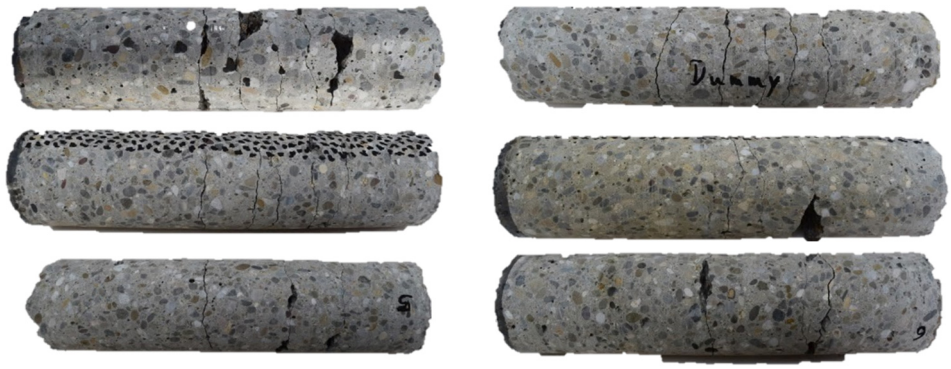

(a) (b)

Figure 7: Fracture specimens after spalling tests under different pressures (from upper to lower rows 1.5, 1 and 0.5 bar). (a) Cylindrical projectile; and (b) Conical projectile.

As already comented in previous paragraphs, the gradual progression of the tensile peak after reflection is one of the advantages obtained from using conical projectiles. This gradual growth of stresses lead to a better determiantion of the first crack in time, and it is well differntiated from the rest. This can be seen when comparing the evolution of the strains in Fig. 8(b). Contrarily, in Fig. 8(a), is clear how in the case of cylindrical projectiles, strains arise into a plateau, leading to a wide portion of the specimen being subjected to similar stress at a certain moment in time, causing simultaneous fractures and complicating the identification of the initial crack.

5.2 Fracture energy tests

Notched specimens were tested under pressure below 0.25 bar, three for each projectile shape. Due to the area reduction at the notched section, similar strain rates were 80–100 s^{-1} determined. Results of the dynamic fracture energy parameters are presented in Table 3. As the specimen is designed to be fractured at the notch, only two fragments are generated. For the measurement of the velocities, two time-instants are considered, t_1 corresponding to the

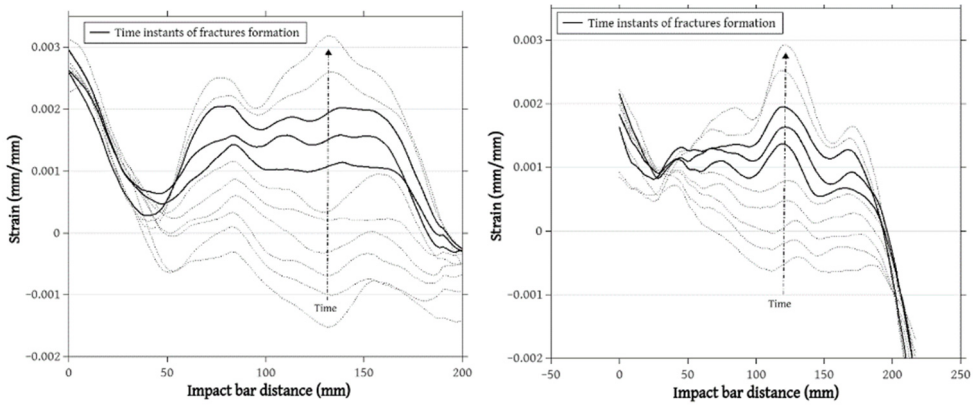

Figure 8: Strain evolution. (a) Cylindrical projectile; and (b) Conical projectile.

moment right before the fracture occurs and t_2 corresponding to the moment just after the fracture. To compute the velocities, in the case of t_1, an analytical procedure was used to derive the velocities of both fragments, while for t_2 velocities were measured using a high-speed extensometer. In the present work, both instants have been measured using a DIC analysis on the images of the high-speed camera. The idea is to obtain a more direct approach to the instant before the fracture.

Table 3: Dynamic fracture energy parameters results.

#Test	$\dot{\varepsilon}$	m_2	ΔI	$\dot{\delta}$	E_F	G_F
	(s^{-1})	(kg)	(kg m/s)	(m/s)	(J)	(N/mm)
Cyl1	86	1.47	1.91	1.52	2.90	1.024
Cyl2	98	1.47	1.62	1.97	3.19	1.127
Cyl3	99	1.48	1.70	2.17	3.69	1.306
Con1	125	1.47	1.87	2.78	5.18	1.832
Con2	85	1.46	1.94	1.46	2.84	1.003
Con3	80	1.50	1.86	1.97	3.65	1.293

Test results show consistency for all performed tested. In test Con1, an alternative configuration to validate the influence of the boundary condition was used. In this case, the specimen was glued to the input bar, ejecting therefore only one part of the specimen after the fracture. An increase in the measured fracture energy for this test can be noted, related either to an inaccurate measurement of the momentum or the increased strain rate for this configuration, but a deeper analysis should be done to clarify this point. From the tests, a mean value of 1.264 N/mm was obtained. Similar values of G_F were obtained between cylindrical and conical projectiles, just a small difference in the higher strain rate produced by the cylindrical projectile. DIF parameter for the fracture energy show that even when the strain rate is kept within a narrow range, a common increasing trend can be seen.

5.3 Dynamic increase factor analysis

As a final point of this research, previous experimental studies are compared with the obtained results. It is important to know wether they fit with literature ones, which have been taken as a reference to check the validity of the results presented.

The dynamic increase factors (DIF) are factors of significant importance in the dynamic analysis of materials and structures, calculated as the ratio of the dynamic to static material parameter, and it is normally defined as the function of strain rate. Fig. 9 presents the DIFs values for different parameters. First, in Fig. 9(a), several tensile strength data for concrete mixtures are compared. The obtainde results in this research are in accordance with the literature data following the well-known trend of linearity till strain rates close to 100 s^{-1}, where the exponential branch with higher values of DIF's starts.

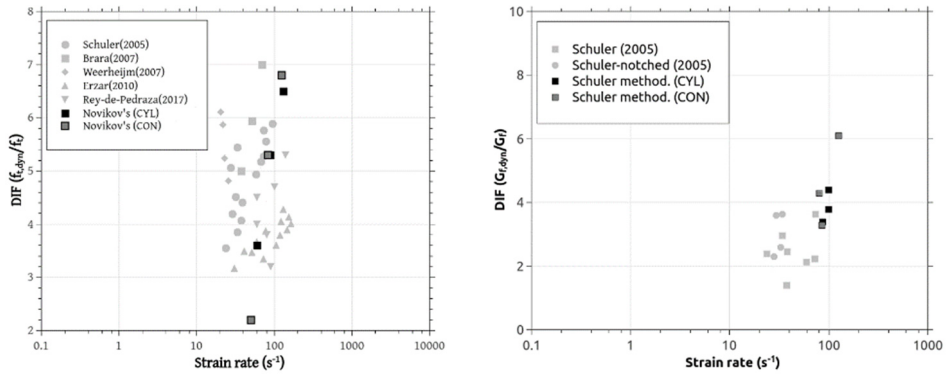

(a) (b)

Figure 9: Comparison between resulted DIF parameter and literature ones. (a) Tensile strength DIF; and (b) Fracture energy DIF. *(Source: Data taken from [14], [25]–[29].)*

Second, in Fig. 9(b) the analysis of different fracture energy values is shown. Due to the similarity of the experimental configuration, the only reference which is considered for the comparison is the work from Schuler et al. [25]. In this case, the comparison complement the founded data, presenting the lack of data with respect to the dynamic fracture energy analysis. As occurred with the dynamic tensile strength, the compared fracture energy shows a common trend for both studies. The critical strain rate seems to be defined at values close to 100 s^{-1}, with a sudden and exponential increase in the fracture energy reached for values of strain rate above that point.

6 CONCLUSIONS

This work presents the evaluation of two main dynamic mechanical properties of concrete: tensile strength and fracture energy. For the evaluation, two different steel projectile were used, a classical cylindrical versus a conical shaped one. The conical projectile was deisgned and validated by numerical simulations.

Dynamic tensile tests were performed using a modified SHB in its spallation configuration. A strain rate dependency was founded for both projectile types. Furhtermore

a qualitative analysis based on the fracture patern reveal the convenience of using conical-projectile geometries for spalling tests. The influence and importance of the projectile's shape on the results was noted on the evolution of strains at the free end of the specimens. Therefore, the introduction of triangular pulse during the tensile loading, lead to a concentration of stresse. The numerical simulation validation allowed aswell to determine the length of the pulse, decreassing the probability of undesired pulse superpositions.

Regarding fracture energy, experiments were performed using notched specimens. As all specimens were brocken by the notch and no diffused damage or extra cracks could be found, the influence of the projectile on the results could not be determined.

ACKNOWLEDGEMENTS

The authors gratefully acknowledge the Ministerio de Ciencia, Innovación y Universidades (MCIU), Agencia Estatal de Investigación (AEI) and Fondo Europeo de Desarrollo Regional (FEDER) for providing financial support for this work under grant PGC2018-097116-A-I00.

REFERENCES

[1] Walley, S.M., The origins of the Hopkinson Bar technique. *The Kolsky-Hopkinson Bar Machine: Selected Topics*, ed. R. Othman, Springer International Publishing: Cham, pp. 1–25, 2018.

[2] Millon, O., Ruiz-Ripoll, M.L. & Hoerth, T., Analysis of the behavior of sedimentary rocks under impact loading. *Rock Mechanics and Rock Engineering*, **49**(11), pp. 4257–4272, 2016. DOI: 10.1007/s00603-016-1010-4.

[3] Birkimer, D.L. & Lindemann, R., Dynamic tensile strength of concrete materials. *Journal Proceedings*, **68**(1), pp. 47–49, 1971. DOI: 10.14359/11293.

[4] Lindholm, U.S. & Yeakley, L.M., High strain-rate testing: Tension and compression. *Experimental Mechanics*, **8**(1), pp. 1–9, 1968. DOI: 10.1007/BF02326244.

[5] Semblat, J.-F., Luong, P. & Gary, G., 3D-Hopkinson Bar: New experiments for dynamic testing on soils. *Soils and Foundations*, **39**, 2009. DOI: 10.3208/sandf.39.1.

[6] Zielinski, A.J. & Reinhardt, H.W., Stress-strain behaviour of concrete and mortar at high rates of tensile loading. *Cement and Concrete Research*, **12**(3), pp. 309–319, 1982. DOI: 10.1016/0008-8846(82)90079-5.

[7] Ožbolt, J., Weerheijm, J. & Sharma, A., Dynamic tensile resistance of concrete: Split Hopkinson bar test. *Proceedings of the 8th International Conference on Fracture Mechanics of Concrete and Concrete Structures, FraMCoS 2013*, pp. 205–216, 2013.

[8] Kolsky, H., An investigation of the mechanical properties of materials at very high rates of loading. *Proceedings of the Physical Society. Section B*, **62**(11), p. 676, 1949. DOI: 10.1088/0370-1301/62/11/302.

[9] Diamaruya, M., Kobayashi, H. & Nonaka, T., Impact tensile strength and fracture of concrete. *Le Journal de Physique IV*, **7**(C3), pp. 253–258, 1997. DOI: 10.1051/jp4:1997345.

[10] Zielinski, A.J. & Reinhardt, H.W., Fracture of concrete and mortar under uniaxial impact tensile loading. PhD thesis, Delft University Press, 1982.

[11] Ross, C.A., Thompson, P.Y. & Tedesco, J.W., Split-Hopkinson pressure-bar tests on concrete and mortar in tension and compression. *Materials Journal*, **86**(5), pp. 475–481, 1989. DOI: 10.14359/2065.

[12] Weerheijm, J., Concrete under impact tensile loading and lateral compression. Delft University, 1992.

[13] Klepaczko, J.R. & Brara, A., An experimental method for dynamic tensile testing of concrete by spalling. *International Journal of Impact Engineering*, **25**(4), pp. 387–409, 2001. DOI: 10.1016/S0734-743X(00)00050-6.
[14] Erzar, B. & Forquin, P., An experimental method to determine the tensile strength of concrete at high rates of strain. *Experimental Mechanics*, **50**(7), pp. 941–955, 2010. DOI: 10.1007/s11340-009-9284-z.
[15] Forquin, P. & Erzar, B., Dynamic fragmentation process in concrete under impact and spalling tests. *International Journal of Fracture*, **163**(1–2), pp. 193–215, 2010. DOI: 10.1007/s10704-009-9419-3.
[16] Dean, A.W., Heard, W.F., Loeffler, C.M., Martin, B.E. & Nie, X., A new Kolsky bar dynamic spall technique for brittle materials. *Journal of Dynamic Behavior of Materials*, **2**(2), pp. 246–250, 2016. DOI: 10.1007/s40870-016-0062-6.
[17] Gálvez Díaz-Rubio, F., Rodríguez Pérez, J. & Sánchez Gálvez, V., The spalling of long bars as a reliable method of measuring the dynamic tensile strength of ceramics. *International Journal of Impact Engineering*, **27**(2), pp. 161–177, 2002. DOI: 10.1016/S0734-743X(01)00039-2.
[18] Rey de Pedraza, V., Ruiz-Ripoll, M.L., Roller, C., Cendón, D.A. & Gálvez, F., Validation of two different analysis techniques to obtain dynamic mechanical properties of concrete using a modified Hopkinson Bar. *International Journal of Impact Engineering*, **161**(1), 104107, 2022. DOI: 10.1016/j.ijimpeng.2021.104107.
[19] C09 Committee, Test method for compressive strength of cylindrical concrete specimens. ASTM International.
[20] RILEM, Determination of the fracture energy of mortar and concrete by means of three-point bend tests on notched beams. 1985. DOI: 10.1007/BF02472918.
[21] Ruiz-Ripoll, M., Millon, O. & Hoerth, T., Dynamic behavior of brittle geological materials under high strain rates. *Anales de la Mecánica de la Fractura*, pp. 178–183, 2015.
[22] Mechtcherine, V., Millon, O., Butler, M. & Thoma, K., Mechanical behavior of SHCC under impact loading. *High Performance Fiber Reinforced Cement Composites 6*, eds G.J. Parra-Montesinos, H.W. Reinhardt & A.E. Naaman, Springer Netherlands: Dordrecht, pp. 297–304, 2012.
[23] Kolsky, H. & Shi, Y.Y., Fractures produced by stress pulses in glass-like solids. *Proceedings of the Physical Society*, **72**, pp. 447–453, 1958. DOI: 10.1088/0370-1328/72/3/317.
[24] Novikov, S.A., Divnov, I.I. & Ivanov, A.G., The study of fracture of steel, aluminium and copper under explosive loading. *Fizika Metallov i Metallovedeniye*, **21**, pp. 608–615, 1966.
[25] Schuler, H., Mayrhofer, C. & Thoma, K., Spall experiments for the measurement of the tensile strength and fracture energy of concrete at high strain rates. *International Journal of Impact Engineering*, **32**(10), pp. 1635–1650, 2006. DOI: 10.1016/j.ijimpeng.2005.01.010.
[26] Brara, A. & Klepaczko, J.R., Experimental characterization of concrete in dynamic tension. *Mechanics of Materials*, **38**(3), pp. 253–267, 2006. DOI: 10.1016/j.mechmat.2005.06.004.
[27] Brara, A. & Klepaczko, J.R., Fracture energy of concrete at high loading rates in tension. *International Journal of Impact Engineering*, **34**(3), pp. 424–435, 2007. DOI: 10.1016/j.ijimpeng.2005.10.004.

[28] Weerheijm, J. & Van Doormaal, J.C.A.M., Tensile failure of concrete at high loading rates: New test data on strength and fracture energy from instrumented spalling tests. *International Journal of Impact Engineering*, **34**(3), pp. 609–626, 2007. DOI: 10.1016/j.ijimpeng.2006.01.005.

[29] Rey-De-Pedraza, V., Cendón, D., Sánchez-Gálvez, V. & Gálvez, F., Measurement of fracture properties of concrete at high strain rates. *Philosophical Transactions of The Royal Society A Mathematical Physical and Engineering Sciences*, **375**, 20160174, 2017. DOI: 10.1098/rsta.2016.0174.